

# Quadrupole deformation signatures in elastic electron scattering from oriented odd- $A$ nuclei

P. Sarriguren

*Instituto de Estructura de la Materia (IEM), CSIC, Serrano 123, E-28006 Madrid, Spain*

---

## Abstract

Elastic electron scattering from oriented odd- $A$  axially deformed nuclei is studied in the plane-wave Born approximation. The nuclear structure is described within a microscopic selfconsistent Skyrme deformed Hartree-Fock approximation with pairing correlations. The interference form factors between monopole and quadrupole Coulomb terms that characterize the nuclear response with aligned nuclear targets are shown to increase or decrease the unpolarized cross-section, depending on the sign of the quadrupole deformation. This feature provides valuable information on the nuclear deformation that can be used as a signature of the oblate or prolate character of the nuclear shape. Some selected cases of nuclei with different spins are presented that exemplify the scope of the method.

*Keywords:* elastic electron scattering, axially deformed nuclei, selfconsistent mean field, charge form factors

---

## 1. Introduction

Nuclear deformation is a crucial piece of information to fully characterize the bulk properties of nuclei [1, 2]. The shape of the nucleus not only determines a large variety of its properties, such as rotational spectra, electromagnetic moments and transition strengths, but it is also essential to understand nuclear decays and reactions with important consequences in other fields. Indeed, the implications of the nuclear shapes extend beyond the realm of nuclear physics itself with impact in nuclear astrophysics and particle physics, where nuclear deformation has been shown to be an important issue to properly understand nuclear reactions and decays in stellar environments [3], as well as rare processes such as the double beta decay [4, 5, 6].

A complete description of the nuclear shape requires in principle a large number of parameters to account for all degrees of freedom. However, a first step to characterize the shape of the nucleus beyond sphericity can be made by assuming axial symmetry and quadrupole deformation. This approximation is still valid to describe properly enough a large variety of the existing nuclei. Neglecting other degrees of freedom, such as triaxiality or higher multipolarities, will not be important for the purpose of this work. The shape of a nucleus with such symmetry is commonly characterized by the quadrupole deformation parameter ( $\beta_2$ ) whose sign indicates whether the axis of symmetry is larger (prolate) or smaller (oblate) than the perpendicular axes. In the former case  $\beta_2$  is positive, in the latter negative.

The nuclear deformation can be theoretically calculated as the shape configuration that minimizes the energy. However, experimental information on the quadrupole deformation parameter and especially its sign, is still limited [7]. In particular, electric quadrupole transition probabilities  $B(E2)$  from the first excited  $2^+$  states in even-even nuclei have been systematically used to get information about the magnitude of  $\beta_2$  [8], but not about its sign because of the quadratic dependence on  $\beta_2$ .

More detailed information about the nuclear structure and specifically about the nuclear shape is provided by Coulomb excitation experiments that simultaneously measure excitation energies and cross-sections [9, 10]. Analysis of the  $\gamma$ -rays in the measured spectrum provides the transition energies between bound states, while the yield of  $\gamma$ -rays with a given energy measures the Coulomb excitation cross-section, which can be related with the electromagnetic transition matrix elements. The development of analytical techniques now available (GOSIA codes) makes it possible to extract detailed information about static moments and relative signs and magnitudes of non-diagonal matrix elements, which allow to determine both the centroids and fluctuation widths of the quadrupole shape degrees of freedom.

Similarly, because the sensitivity of the  $\beta$ -strength distribution to deformation,  $\beta$ -decay experiments have also been proposed as a complementary tool to obtain information about the nuclear shape of unstable nuclei [11, 12].

An alternative method to get information on the sign of the quadrupole deformation that has not been sufficiently explored yet is to use the sensitivity of the electron scattering experiments to the nuclear charge density distribution and, as a result, to the nuclear deformation. The electron

---

*Email address:* p.sarriguren@csic.es (P. Sarriguren)

scattering cross-section contains the information of the full charge density distribution of the nucleus, which appears through the charge form factors [13, 14, 15, 16].

The relationship between the charge form factors and the properties that characterize the charge density distributions has been studied within different approaches that include the Shell Model [17, 18], as well as relativistic [19, 20, 21, 22, 23, 24, 25] and nonrelativistic [26, 27, 28, 29, 30] selfconsistent mean-field models. All these models show clear correlations between them. In particular, the value of the momentum transfer at the first minimum of the charge form factor is related with the r.m.s. radius of the charge distribution [19, 20, 21, 28], whereas the height of the second maximum is related with the surface diffuseness of the charge distribution [28, 29, 31].

Isotopic and isotonic chains have been studied in the above mentioned works to stress different aspects of nuclear structure. Isotopic chains are useful to study the effect of neutrons on the charge density that becomes more diluted as the number of neutrons increases. Similarly, the effect of the outer protons can be analyzed in isotonic chains and details of the proton wave functions can be studied. An upward and inward shift of the diffraction minima of the charge form factors is found with increasing nucleon number in both type of chains.

The Coulomb form factors for deformed nuclei can be expressed in terms of multipoles  $C\lambda$  [15, 32], which are sensitive to the different components of a multipolar decomposition of the deformed charge density distribution. In particular, the  $C0$  component would contain the information on the dominant spherical component, whereas the  $C2$  component would contain the information on the quadrupole nuclear deformation. However, in traditional electron scattering, where unpolarized electron beams are scattered from unpolarized nuclear targets, the total charge form factor appears as an incoherent sum of multipoles squared. Therefore, the information sensitive to the nuclear deformation is hidden because of two main reasons. First, the contributions from higher multipolarities to the cross-section rapidly become smaller with increasing multipolarity. Second, only the square of  $C2$  multipoles contributes and this prevents extracting information about the sign that determines the oblate or prolate character of the deformation.

The combined effects of both quadrupole deformation and r.m.s. radii on the diffraction minima of the charge form factors have also been studied [22, 23, 24, 25, 30]. However, because of the above reasons, information on the nuclear deformation is difficult to be disentangled. For example, it has been shown [23] that in ordinary electron scattering  $C2$  contributions manifest significantly only at the  $C0$  diffraction minima, but unfortunately, this occurs at relatively large momentum transfer, where the form factors are small and difficult to measure.

One possible way to solve this problem is the use polarization degrees of freedom in the electron scattering from

nuclei [32, 33, 34]. In this case, new observables appear that contain interference terms between the various multipoles that can be isolated experimentally with proper choices of the directions of both scattered electrons and nuclear polarizations. In particular, interference terms between longitudinal multipoles  $C0/C2$  appear in the case of scattering from unpolarized electrons from oriented nuclei and they will be the focus in this work. These interference terms are much larger than the  $C2$  squared terms that characterize the unpolarized cross-sections and involve phases sensitive to the quadrupole sign that increase or decrease significantly the unpolarized cross-sections. The essential point is that new combinations of the form factors (other than incoherent sums of squares) can be measured by varying the polarization direction of the nucleus.

In the simplest realization of these experiments, polarized internal targets are located to intercept the circulating electrons in storage rings. The high currents achieved in these storage rings allow the use of thin targets that can be more easily polarized, reaching luminosities comparable with those in conventional experiments [35, 36]. New possibilities with unprecedented polarization quality of both electron and ion beams are also expected in the new generations of facilities, in particular, in the Electron-Ion Collider at Brookhaven National Laboratory [37].

Most of the scattering experiments in the past were carried out with stable nuclei. In this work we focus on examples among them. However, this could change soon with the setup of collider experiments with electrons and radioactive ion beams. The SCRIT project at RIKEN [38, 39] and the ELISE project planned for the GSI-FAIR [38, 40] are examples of these new facilities.

In the next section the theoretical formalism used to describe the reaction mechanism and the nuclear structure of the electron scattering from deformed aligned odd- $A$  nuclei is presented. Section 3 contains the results of this study on the examples of  $^{23}\text{Na}$ ,  $^{25}\text{Mg}$ , and  $^{59}\text{Co}$ . The main conclusions are shown in the last section.

## 2. FORMALISM

The reaction mechanism used in this work is based on the plane wave Born approximation (PWBA) that assumes one-photon exchanged and plane waves for the electrons. In addition to the numerical advantage, PWBA relates directly the charge form factors with the Fourier transforms of the charge matrix elements and the physical interpretation is straightforward. Coulomb distortion effects evaluated from the distorted wave Born approximation (DWBA) will be needed for a final comparison with experiment. They can be included within a phase-shift analysis [41]. However, the main effects of Coulomb distortion are the filling of the diffraction minima and a shift of their locations. These effects are small at low momentum transfer ( $q \leq 1.2 \text{ fm}^{-1}$ ), where the effects from target orientation are already significant.

The theoretical formalism for inclusive electron-nucleus scattering involving polarization degrees of freedom in both beams and targets has been developed elsewhere [33, 34] and has been particularized to the case of deformed nuclei in Refs. [32, 42]. Here, we only summarize the most relevant results regarding the nuclear longitudinal ( $L$ ) response functions (also known as charge or Coulomb responses) for experiments dealing with polarized targets without measuring electron polarizations. Similar results can be obtained in the case where the target is not polarized, but the polarization of the final nucleus is measured. The longitudinal response can always be separated from the transverse one that involves electric and magnetic contributions by a Rosenbluth analysis, using the dependence of the different weighting factors on the electron kinematics.

Following the notation in Ref. [32], the electron scattering cross-section in PWBA from deformed oriented nuclei with a ground state  $I_i^{\pi_i}$  characterized by spin  $I_i$  and parity  $\pi_i$  to a final state  $I_f^{\pi_f}$  is given by

$$\frac{d\sigma}{d\Omega} \Big|_{I_i^{\pi_i} \rightarrow I_f^{\pi_f}} = \sigma_{\text{tot}}(\theta', \phi') = Z^2 \sigma_M f_{\text{rec}}^{-1} [\sigma_0 + \sigma_{\text{al}}(\theta', \phi')] , \quad (1)$$

where  $\sigma_M$  is the Mott cross-section,  $f_{\text{rec}}$  the recoil factor, and the angles  $(\theta', \phi')$  represent the polarization direction of the target relative to the system determined by the momentum transfer  $\vec{q} = \vec{k}_i - \vec{k}_f$ . Figures showing the relationship between the target polarization direction, the  $\vec{q}$ -system and the laboratory system can be found in Ref. [32].

The cross-section  $\sigma_0$  does not depend on polarizations and is given by

$$\sigma_0 = V_L |F_L(q)|^2 + V_T |F_T(q)|^2 . \quad (2)$$

$V_L$  and  $V_T$  are kinematical factors given by

$$V_L = (Q^2/q^2)^2 , \quad V_T = \tan^2(\theta_e/2) - (Q^2/q^2)/2 , \quad (3)$$

where  $Q^\mu = (\omega, \vec{q})$  is the four-momentum transferred to the nucleus in the process in which an incoming electron with four-momentum  $k_i^\mu = (\varepsilon_i, \vec{k}_i)$  is scattered through an angle  $\theta_e$  to an outgoing electron with four-momentum  $k_f^\mu = (\varepsilon_f, \vec{k}_f)$ , with  $\omega = \varepsilon_i - \varepsilon_f$  and  $\vec{q} = \vec{k}_i - \vec{k}_f$ .  $F_L$  and  $F_T$  are the longitudinal and transverse form factors that contain the nuclear structure information in terms of charge ( $L$ ) and electric and magnetic ( $T$ ) multipoles. These contributions can be isolated with proper choices of the kinematical variables using Rosenbluth separation methods. The focus here is on the Coulomb response  $F_L(q)$  that can be written in terms of the charge multipole form factors  $F^{C\lambda}(q)$

$$|F_L(I_i, I_f; q)|^2 = \sum_{\lambda \geq 0} |F^{C\lambda}(I_i, I_f; q)|^2 . \quad (4)$$

The various multipole contributions add incoherently and share the same factors in the cross-section, making it impossible to separate them kinematically. The multipole charge form factors are given by

$$F^{C\lambda}(I_i, I_f; q) = \frac{\sqrt{4\pi}}{Z} \langle I_f | \hat{T}^{C\lambda}(q) | I_i \rangle / \sqrt{2I_i + 1} , \quad (5)$$

where the Coulomb multipole operators are

$$\hat{T}_\mu^{C\lambda}(q) = i^\lambda \int d\mathbf{R} j_\lambda(qR) Y_\lambda^\mu(\Omega_R) \hat{\rho}(\mathbf{R}) , \quad (6)$$

in terms of the nuclear charge operator  $\hat{\rho}(\mathbf{R})$ .

Similarly,  $\sigma_{\text{al}}$  is independent of projectile polarizations and depends on the orientation of the target.

$$\begin{aligned} \sigma_{\text{al}}(\theta', \phi') = & \sum_{\ell=\text{even}>0} \alpha_\ell^{I_i} [P_\ell(\cos \theta') (-V_L F_L^\ell + V_T F_T^\ell) \\ & + P_\ell^2(\cos \theta') \cos(2\phi') V_{TT} F_{TT}^\ell \\ & + P_\ell^1(\cos \theta') \cos \phi' V_{TL} F_{TL}^\ell] . \end{aligned} \quad (7)$$

$V_{TT}$  and  $V_{TL}$  are kinematical factors whose explicit expressions can be found in Ref. [32]. The terms  $TT$  and  $TL$  are not considered further in this work because they do not contribute to the cross-section when the nuclei are oriented in the  $\theta' = 0$  direction, which will be the only case considered here.

The structure functions  $F$ 's contain different interference terms that can be separated using the dependence on the polarization direction  $(\theta', \phi')$ , the statistical factors  $\alpha_\ell^{I_i}$ , and the dependence on the scattering angle  $\theta_e$ . In particular, the interest of this work focuses on the interference between longitudinal multipoles that are contained in the term  $F_L^\ell$ .

The statistical tensors describe the orientation of the target, reflecting that the  $2I_i + 1$  substates are not equally populated,

$$\alpha_\ell^{I_i} = \sum_{M_i} P(M_i) \langle I_i M_i \ell 0 | I_i M_i \rangle , \quad (8)$$

where  $P(M_i)$  are the occupation probabilities of the target substates  $|I_i M_i\rangle$  along the polarization direction  $(\theta', \phi')$ . They are defined so that for  $\ell = 0$  one has  $\alpha_{\ell=0}^{I_i} = 1$  regardless of the state of polarization. For unpolarized targets where  $P(M_i) = 1/(2I_i + 1)$ , one has  $\alpha_\ell^{I_i} = \delta_{\ell,0}$ . In the case of aligned nuclei,  $P(M_i) = P(-M_i)$ , all the statistical tensors with odd values of  $\ell$  vanish. In those cases the use of polarized electrons is irrelevant.

The form factors  $F_L^\ell$  contain interference terms between the different Coulomb multipoles:

$$F_L^\ell(I_i, I_f; q) = \sum_{\lambda, \lambda'} X(\lambda, \lambda', I_i, I_f, \ell) F^{C\lambda}(I_i, I_f; q) F^{C\lambda'}(I_i, I_f; q) , \quad (9)$$

where  $X(\lambda, \lambda', I_i, I_f, \ell)$  are geometrical factors involving 3j- and 6j- Wigner coefficients [32],

$$X = (-1)^{I_i + I_f + 1} \bar{I}_i \bar{\lambda} \bar{\lambda}' \bar{\ell}^2 \begin{pmatrix} \lambda & \lambda' & \ell \\ 0 & 0 & 0 \end{pmatrix} \left\{ \begin{matrix} I_i & I_i & \ell \\ \lambda & \lambda' & I_f \end{matrix} \right\}, \quad (10)$$

with  $\bar{a} = \sqrt{2a + 1}$ .

The transition multipole charge form factors  $F^{C\lambda}(I_i, I_f; q)$  corresponding to a given transition  $I_i k \rightarrow I_f k$  within a rotational band characterized by the spin projection along the symmetry axis  $k$ , can be written up to lowest order in angular momentum [32] in terms of intrinsic form factors

$$F^{C\lambda}(I_i, I_f; q) = \langle I_i k \lambda 0 | I_f k \rangle \mathcal{F}^{C\lambda}(q). \quad (11)$$

They are given by

$$\mathcal{F}^{C\lambda}(q) = i^\lambda \sqrt{\frac{4\pi}{2\lambda + 1}} \int_0^\infty R^2 dR \rho_\lambda(R) j_\lambda(qR), \quad (12)$$

where  $\rho_\lambda(R)$  are the multipole components of an expansion of the density  $\rho(\mathbf{R})$  in Legendre polynomials,

$$\rho_\lambda(R) = (2\lambda + 1) \int_0^{\pi/2} P_\lambda(\cos\theta) \rho(R \cos\theta, R \sin\theta) d(\cos\theta), \quad (13)$$

Note that in axially symmetric nuclei the density depends only on two coordinates,  $R \cos\theta$  and  $R \sin\theta$ .

In all the calculations in this work, center of mass corrections are considered in the harmonic-oscillator approximation, including a factor  $\exp[q^2/(4A^{2/3})]$ . Nucleon finite size effects are included as a sum of monopoles parametrized in Ref. [43] for the proton and by the difference of two Gaussians [44] for the neutron.

The nuclear structure used to describe the nuclear densities needed for the calculations of the different multipole charge form factors are obtained within a deformed Skyrme (SLy4) Hartree-Fock (HF) with pairing correlations in the BCS approximation, as described in Ref. [45]. In this formalism, the nuclear density is given by

$$\rho(\mathbf{R}) = 2 \sum_i v_i^2 |\Phi_i(\mathbf{R})|^2, \quad (14)$$

in terms of the occupation probabilities  $v_i^2$  and the single-particle Hartree-Fock wave functions  $\Phi_i$ , which are expanded into the eigenstates of an axially deformed harmonic oscillator potential [45]. The quadrupole deformation  $\beta_2$  is obtained selfconsistently from the intrinsic quadrupole moment  $Q_0$  and the mean square radius  $\langle R^2 \rangle$ , both calculated microscopically in terms of the density,

$$\begin{aligned} \beta_2 &= \sqrt{\frac{\pi}{5}} \frac{Q_0}{A \langle R^2 \rangle}, \\ Q_0 &= \sqrt{16\pi/5} \int \rho(\vec{R}) R^2 Y_{20}(\Omega_R) d\vec{R}, \\ \langle R^2 \rangle &= \frac{\int R^2 \rho(\vec{R}) d\vec{R}}{\int \rho(\vec{R}) d\vec{R}}. \end{aligned} \quad (15)$$

This formalism to describe axially deformed nuclei has been used in the past for the calculation of both longitudinal and transverse form factors [46, 47, 48, 49, 50, 51, 52].

The main objective of the present work is the study of the interference between the monopole  $C0$  and quadrupole  $C2$  charge form factors, as contained in Eq. (9). For even-even rotators ( $I = k = 0$ ) there is no possibility of target orientation. In this case, information on the  $C2$  multipoles can only be extracted as  $|F^{C2}|^2$  from ordinary inelastic transitions to the  $2^+$  excited states that prevents getting information about the sign of deformation. Things are different for odd- $A$  rotors that can be aligned. In this case, only elastic scattering will receive  $C0$  contributions. Therefore, the focus here is on the elastic scattering from odd- $A$  aligned nuclei with  $I = k \geq 3/2$ , where  $C0$  and  $C2$  multipoles are involved and their interference will contribute to the cross-section. In the case of elastic scattering  $I_i = I_f$ , the notation of the charge multipoles is simplified to  $F^{C\lambda}(I_i = I_f, I_f; q) \equiv F_{I_f}^{C\lambda}(q)$ .

Nuclei with  $I = k = 1/2$  cannot be aligned because they could not be distinguished from the unpolarized case. In addition, elastic scattering from them will not receive  $C2$  contributions, whereas inelastic transitions will not be sensitive to the  $C0$ . Therefore, for  $k_i = 1/2$  nuclei, only the special case where the ground state is given by  $I_i = 3/2$ , which is possible because of Coriolis effects, will receive  $C0/C2$  interferences. This case has already been discussed in Refs. [32, 42].

The key point is that by measuring both the unpolarized and the polarized cross-sections, one can see whether the target polarization increases or decreases the former, being a model independent signature of the oblate or prolate character of the deformed target.

The form factors containing interference terms can be experimentally separated with measurements of the cross-sections at  $\theta' = 0$ , that is, with nuclei oriented in the  $\vec{q} = \vec{k}_i - \vec{k}_f$  direction

$$\sigma_{\text{tot}}(\theta' = 0, \phi') - \sigma_0 = \sum_\ell \alpha_\ell^{I_i} (-V_L F_L^\ell + V_T F_T^\ell) \quad (16)$$

and using the kinematical dependence of the  $V_L$  and  $V_T$  factors, the contribution from  $F_L^\ell$  containing the interference of different charge multipoles can be isolated and studied separately. The focus here is on the  $C0/C2$  interferences that appear in the  $\ell = 2$  terms,

$$\sigma_{\text{al}} = -\alpha_2^{I_i} P_2(\cos\theta') V_L F_L^{\ell=2}. \quad (17)$$

The  $X$  coefficient in Eqs. (9) and (10), in the elastic case  $I_i = I_f = k$ , and for  $\ell = 2$  involving the  $C0/C2$  interference terms is given by  $X = -2\sqrt{5}$ , independent of the spin values. Then,

$$F_L^{\ell=2}(I_f; q) = -2\sqrt{5}F_{I_f}^{C0}(q)F_{I_f}^{C2}(q). \quad (18)$$

This form factor contains information about the relative phase of  $C0$  and  $C2$  multipole form factors and therefore, about the sign of the quadrupole charge multipole  $\rho_2$ . This goes beyond the possibilities of ordinary electron scattering, where the Coulomb contribution is given by

$$\sigma_0 = V_L|F_L|^2 = V_L \left( |F_{I_f}^{C0}|^2 + |F_{I_f}^{C2}|^2 + \mathcal{O}(C\lambda \geq 4) \right). \quad (19)$$

For aligned nuclei with  $P(M_i = +I_i) = P(M_i = -I_i) = 0.5$ , or similarly for fully polarized nuclei  $P(M_i) = \delta_{M_i, +I_i}$ , the statistical tensors  $\alpha_2^{I_i}$  in Eq. (8) are given by  $1/\sqrt{5}$ ,  $\sqrt{5/14}$ , and  $\sqrt{7/15}$ , for  $I_i = 3/2$ ,  $5/2$ , and  $7/2$ , respectively.

The transition form factors can be written in terms of the intrinsic form factors with the Clebsh-Gordan coefficients in Eq. (11). The resulting interference form factors  $F_L^{\ell=2}$  (9), in terms of the intrinsic form factors  $\mathcal{F}^{C0}$  and  $\mathcal{F}^{C2}$  are given by

$$F_L^{\ell=2}(I_f; q) = \mathcal{A}(I_f)\mathcal{F}^{C0}(q)\mathcal{F}^{C2}(q), \quad (20)$$

with  $\mathcal{A} = -2$ ,  $-5/7$ , and  $-2\sqrt{7/3}$ , for  $I_i = I_f = 3/2$ ,  $5/2$ , and  $7/2$ , respectively.

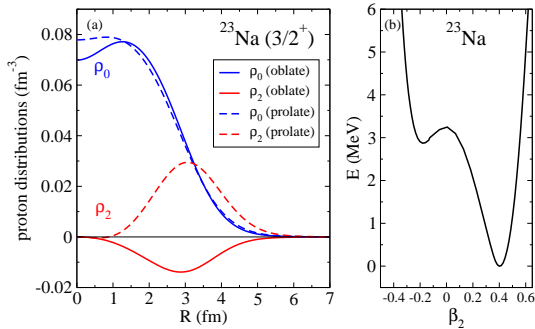


Figure 1: (a) Multipole components of the proton distributions in  $^{23}\text{Na}$  ( $I = k = 3/2$ ) for the oblate and prolate shape configurations. (b) Excitation energy as a function of the quadrupole parameter  $\beta_2$ .

### 3. Results

In this section, the results for the multipole form factors and interferences are presented on the example of some selected deformed and stable nuclei. Specifically, we study  $^{23}\text{Na}$  ( $I_{\text{g.s.}}^\pi = 3/2^+$ ),  $^{25}\text{Mg}$  ( $I_{\text{g.s.}}^\pi = 5/2^+$ ), and  $^{59}\text{Co}$  ( $I_{\text{g.s.}}^\pi = 7/2^-$ ).

Figures 1, 2, and 3 contain the results for the multipole densities  $\rho_0$  and  $\rho_2$  for the proton distributions in  $^{23}\text{Na}$ ,  $^{25}\text{Mg}$ , and  $^{59}\text{Co}$ , respectively, as well as the ground-state

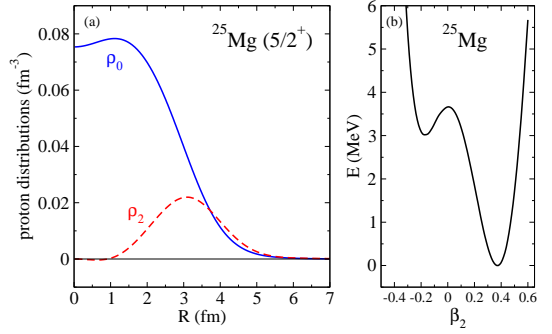


Figure 2: Same as in Figure 1, but for the prolate shape in  $^{25}\text{Mg}$  ( $I = k = 5/2$ ).

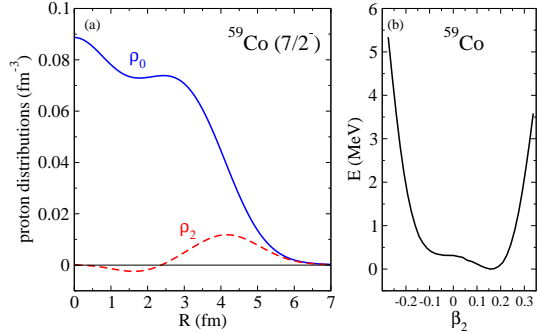


Figure 3: Same as in Figure 1, but for the prolate shape in  $^{59}\text{Co}$  ( $I = k = 7/2$ ).

energies as a function of the quadrupole deformation parameter  $\beta_2$ , defined in Eq. (15). In the case of  $^{23}\text{Na}$ , both prolate and oblate deformations are considered for the calculations since both minima correspond to  $3/2^+$  states in agreement with the experimental assignment. In the other two cases only the prolate shape is studied because the spin-parities match the experiment,  $5/2^+$  in  $^{25}\text{Mg}$  and  $7/2^-$  in  $^{59}\text{Co}$ , while the oblate minima correspond to different states. From these figures one can see that  $\rho_2(R)$  mainly peaks in the surface region, being positive or negative depending on the sign of deformation. On the other hand, the density does not change much in the nuclear interior. This sign difference will manifest itself in the  $C2$  form factors becoming a signature of the oblate/prolate character of the nuclear shape.

The next figures, 4 and 5, contain the Coulomb form factors squared  $(F_{I_f}^{C0})^2$ ,  $(F_{I_f}^{C2})^2$ , and  $F_L^{\ell=2}$ . Figure 4 shows the results for the oblate and prolate shapes in  $^{23}\text{Na}$ , while figure 5 shows the results for the prolate shape in  $^{25}\text{Mg}$  and  $^{59}\text{Co}$ . Plus or minus signs under the peaks of the form factors squared indicate the sign of the corresponding multipole form factor  $F_{I_f}^{C\lambda}$ .

From these figures one can appreciate the obvious difficulty to extract information on  $C2$  multipoles from unpolarized experiments. First, because of their small magnitude compared to  $C0$ , which means that they only manifest significantly at diffraction minima. Secondly, because only the squared  $(F^{C2})^2$  are measurable and therefore, no

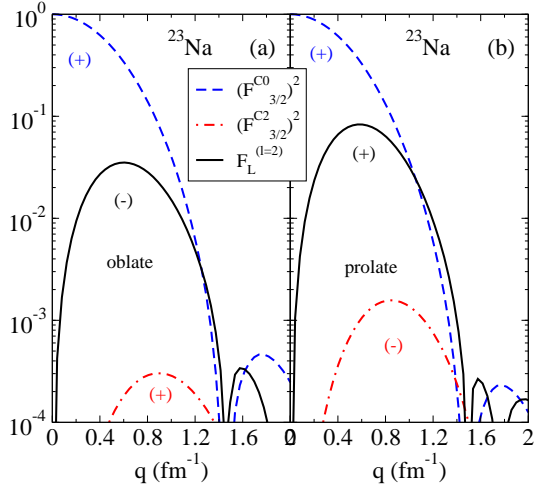


Figure 4: (a)  $(F_{3/2}^{C\lambda})^2$  and  $F_L^{\ell=2}$  form factors for the oblate shape in  $^{23}\text{Na}$ . (b) Same for the prolate shape. Signs under the peaks in  $(F_{3/2}^{C\lambda})^2$  show the sign of the multipoles  $F_{3/2}^{C\lambda}$ .

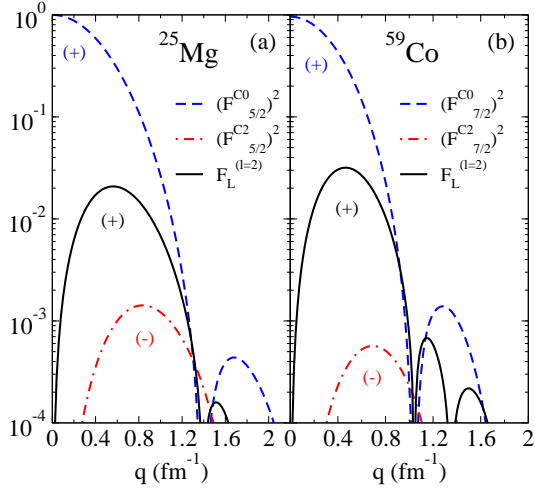


Figure 5: Same as in Figure 4, but for the prolate shapes of (a)  $^{25}\text{Mg}$  ( $F_{5/2}^{C\lambda}$ ) and (b)  $^{59}\text{Co}$  ( $F_{7/2}^{C\lambda}$ ).

information about the sign of  $\rho_2$  can be extracted. On the other hand, the interference term  $F_L^{\ell=2}$  is much larger than  $(F^{C2})^2$  and contains information of the sign of deformation. Since the terms  $F_L^{\ell=2}$  can be experimentally isolated, their comparison with the usual  $(F^{C0})^2$  and  $(F^{C2})^2$  form factors is of great interest. Typically, the first peak of  $F_L^{\ell=2}$  is about one order of magnitude smaller than  $(F^{C0})^2$  and one order of magnitude larger than  $(F^{C2})^2$ .

Under the conditions established in Section 2, the longitudinal contribution to the cross-section can be written as

$$\sigma_{\text{tot}} = \sigma_0 + \sigma_{\text{al}} \sim V_L F_{\text{eff}}, \quad (21)$$

where

$$F_{\text{eff}} = |F_L|^2 + F_{02} = |F^{C0}|^2 + |F^{C2}|^2 + F_{02}, \quad (22)$$

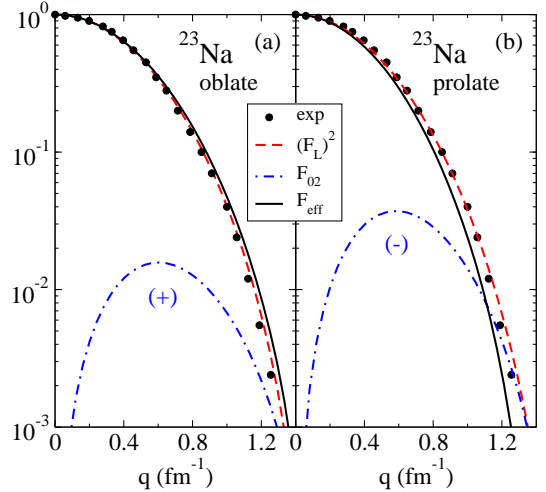


Figure 6:  $(F_L)^2$ ,  $F_{02}$ , and  $F_{\text{eff}}$  form factors in  $^{23}\text{Na}$ , (see text) for oblate (a) and prolate (b) shapes. Experimental data for the unpolarized form factor  $(F_L)^2$  are taken from [23, 53].

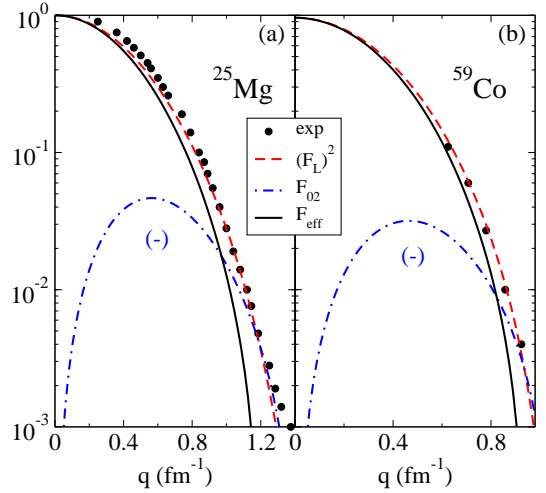


Figure 7: Same as in Figure 6, but for the prolate shapes in  $^{25}\text{Mg}$  (a) and  $^{59}\text{Co}$  (b). Experimental data are taken from [23, 54, 55].

with

$$F_{02} = -\alpha_2^i P_2(\cos \theta') F_L^{(\ell=2)}. \quad (23)$$

Figures 6 and 7 contain the total calculated and measured longitudinal form factor  $(F_L)^2 = (F^{C0})^2 + (F^{C2})^2$  in the unpolarized case, together with the above defined  $F_{02}$  and  $F_{\text{eff}}$  form factors for  $^{23}\text{Na}$  oblate and prolate and for prolate shapes in  $^{25}\text{Mg}$  and  $^{59}\text{Co}$ . Comparing the unpolarized response, which is proportional to  $(F_L)^2$  with the polarized one, which is proportional to  $F_{\text{eff}}$ , one can see that simply measuring both the unpolarized and polarized cross-sections and checking whether it increases or decreases, information on the oblate or prolate type of the nuclear shape can be inferred. This relative comparison of cross-sections would give us a model independent signature of the sign of deformation. Further isolation of  $F_L^{(\ell=2)}$  will provide more detailed information about  $\rho_2$ .

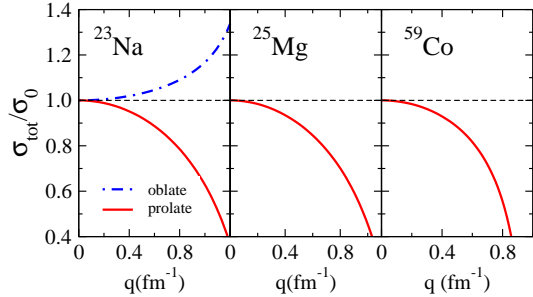


Figure 8: Ratio between the total cross-section with aligned nuclei and the unpolarized one.

Figure 8 shows the ratio between the total polarized cross-section with aligned nuclei and the unpolarized one,

$$\frac{(\sigma_0 + \sigma_{\text{al}})}{\sigma_0} = 1 + \frac{F_{02}}{|F_L|^2} = \frac{F_{\text{eff}}}{|F_L|^2}. \quad (24)$$

It clearly shows the magnitude of the deviation from the standard unpolarized cross-section. The change begins to be significant already at low momentum transfer and becomes sizable below the first diffraction minimum, where the cross-section is large enough to be measured. In the neighborhood of the minimum the cross-section is very small and other effects not taken into account in this study may appear.

#### 4. Conclusions

The effect of deformation on the interference form factors between monopole and quadrupole Coulomb terms, and therefore, on the total electron-scattering cross-section has been studied in odd- $A$  nuclei. Examples of the magnitude of the expected effects are shown in specific cases with different spin-parity ground states, namely,  $^{23}\text{Na}$  ( $I^\pi = 3/2^+$ ),  $^{25}\text{Mg}$  ( $I^\pi = 5/2^+$ ), and  $^{59}\text{Co}$  ( $I^\pi = 7/2^-$ ). In this work, the focus is placed on elastic scattering with unpolarized electrons, but with oriented odd- $A$  axially deformed nuclei. The reaction mechanism is based on the PWBA, whereas the nuclear structure is described with selfconsistent Skyrme HF+BCS calculations.

A more systematic and general study of the interferences between different multipoles, without the restrictions made in this work will be performed in a forthcoming publication [56], where issues like inelastic reactions, polarized electrons, higher spins, Coulomb distortions, or interferences other than  $C_0/C_2$  will be considered. It will be also interesting to study the sensitivity of the cross-section to the nuclear shape in nuclei exhibiting shape coexistence, where oblate and prolate configurations have similar energies. The present study provides clues about the different effects expected from oblate or prolate shapes.

The limitations imposed in this work do not alter the final conclusions regarding the possibility of measuring observables, which are sensitive to the  $C_0/C_2$  interference

and, as a consequence, are sensitive to the sign of the axial deformation in odd- $A$  nuclei. This model independent signature appears as an increase or decrease of the unpolarized cross-section. The magnitude of such effect will depend on the particular nuclear model used.

#### Acknowledgments

This work was supported by Grant PGC2018-093636-B-I00, funded by MCIN/AEI/10.13039/501100011033 and by ERDF 'A way of making Europe'.

#### References

- [1] A. Bohr and B. Mottelson, *Nuclear Structure*, (Benjamin, New York 1975).
- [2] P. Ring and P. Schuck, *The Nuclear Many Body Problem*, (Springer, 2004).
- [3] P. Sarriguren, Phys. Lett. B 680 (2009) 438; Phys. Rev. C 83 (2011) 025801.
- [4] A. A. Raduta, A. Escuderos, Amand Faessler, E. Moya de Guerra, and P. Sarriguren, Phys. Rev. C 69 (2004) 064321.
- [5] R. Alvarez-Rodriguez, P. Sarriguren, E. Moya de Guerra, L. Paceaescu, Amand Faessler, and F. Simkovic, Phys. Rev. C 70 (2004) 064309.
- [6] D. L. Fang, A. Faessler, V. Rodin, and F. Simkovic, Phys. Rev. C 83 (2011) 034320.
- [7] N.J. Stone, At. Data and Nucl. Data Tables 90 (2005) 75.
- [8] B. Pritychenko, M. Birch, B. Singh, and M. Horoi, At. Data and Nucl. Data Tables 107 (2016) 1.
- [9] T. Glasmacher, Ann. Rev. Nucl. Part. Sci. 48 (1998) 1.
- [10] D. Cline, Ann. Rev. Nucl. Part. Sci. 36 (1986) 683.
- [11] E. Nacher, et al., Phys. Rev. Lett. 92 (2004) 232501.
- [12] P. Sarriguren, Phys. Rev. C 91 (2015) 044304.
- [13] R. Hofstadter, Rev. Mod. Phys. 28 (1956) 214.
- [14] T. de Forest and J. D. Walecka, Ad. Phys. 15 (1966) 1.
- [15] T. W. Donnelly and J. D. Walecka, Ann. Rev. Nucl. Sci. 25 (1975) 329.
- [16] J. Heisenberg and H. P. Blok, Ann. Rev. Nucl. Sci. 33(1983) 569.
- [17] B.A. Brown, R. Radhi, and B.H. Wildenthal, Phys. Rep. 101 (1983) 313.
- [18] R. A. Radhi, A. A. Alzubadi, and A. H. Ali, Phys. Rev. C 97 (2018) 064312; R. A. Radhi, A. A. Alzubadi, and N. S. Manie, Nucl. Phys. A 1015 (2021) 122302.
- [19] Z. Wang and Z. Ren, Phys. Rev. C 71 (2005) 054323.
- [20] X. Roca-Maza, M. Centelles, F. Salvat, and X. Viñas, Phys. Rev. C 78 (2008) 044332.
- [21] X. Roca-Maza, M. Centelles, F. Salvat, and X. Viñas, Phys. Rev. C 87 (2013) 014304.
- [22] J. Liu, C. Xu, and Z. Ren, Phys. Rev. C 95 (2017) 044318.
- [23] J. Liu, C. Xu, S. Wang, and Z. Ren, Phys. Rev. C 96 (2017) 034314.
- [24] T. Liang, J. Liu, Z. Ren, C. Xu, and S. Wang, Phys. Rev. C 98, (2018) 044310.
- [25] J. Liu, R. Xu, J. Zhang, C. Xu, and Z. Ren, J. Phys. G: Nucl. Part. Phys. 46 (2019) 055105.
- [26] W. A. Richter and B. A. Brown, Phys. Rev. C 67 (2003) 034317.
- [27] A. N. Antonov, D. N. Kadrev, M. K. Gaidarov, E. Moya de Guerra, P. Sarriguren, J. M. Udias, V. K. Lukyanov, E. V. Zemlyanaya, and G. Z. Krumova, Phys. Rev. C 72 (2005) 044307.
- [28] P. Sarriguren, M. K. Gaidarov, E. Moya de Guerra, and A. N. Antonov, Phys. Rev. C 76 (2007) 044322.
- [29] J. M. Yao, M. Bender, and P.-H. Heenen, Phys. Rev. C 91 (2015) 024301.

- [30] L. Wang, J. Liu, T. Liang, Z. Ren, C. Xu, and S. Wang, *J. Phys. G: Nucl. Part. Phys.* 47 (2020) 025105.
- [31] J. Friedrich and N. Voegler, *Nucl. Phys. A* 373 (1982) 192.
- [32] E. Moya de Guerra, *Phys. Rep.* 138 (1986) 293.
- [33] L. J. Weigert and M. E. Rose, *Nucl. Phys.* 51 (1964) 529.
- [34] T. W. Donnelly and A. S. Raskin, *Ann. of Phys.* 169 (1986) 247.
- [35] Proc. of the Workshop on Polarized Targets in Storage Rings, Ed. R.J. Holt, Argonne National Lab, ANL-84-50 (1984).
- [36] E. Passchier et al., *Nucl. Inst. Meth. A* 387 (1997) 471; M. Ferro-Luzzi et al., *Nucl. Phys. A* 654 (1999) 1009c.
- [37] Science Requirements and Detector Concepts for the Electron-Ion Collider: EIC Yellow Report (2021). *Nucl. Phys. A* 1026 (2022) 122447.
- [38] T. Suda and H. Simon, *Prog. Part. Nucl. Phys.* 96 (2017) 1.
- [39] K. Tsukada *et al.*, *Phys. Rev. Lett.* 118 (2017) 262501.
- [40] A. N. Antonov *et al.*, *Nucl. Inst. and Meth. A* 637 (2011) 60.
- [41] D. R. Yennie, D. G. Ravenhall, and R. N. Wilson, *Phys. Rev.* 95 (1954) 500.
- [42] E. Garrido, E. Moya de Guerra, P. Sarriguren, and J.M. Udias, *Nucl. Phys. A* 550 (1992) 391.
- [43] G. G. Simon, Ch. Schmitt, F. Borkowski, and V. H. Walther, *Nucl. Phys. A* 333 (1980) 381.
- [44] H. Chandra and G. Sauer, *Phys. Rev. C* 13 (1976) 245.
- [45] D. Vautherin, *Phys. Rev. C* 7 (1973) 296.
- [46] E. Moya de Guerra and S. Kowalski, *Phys. Rev. C* 22 (1980) 1308.
- [47] D. Berdichevsky, P. Sarriguren, E. Moya de Guerra, M. Nishimura, and D. W. L. Sprung, *Phys. Rev. C* 38 (1988) 338.
- [48] E. Graca, P. Sarriguren, D. Berdichevsky, D. W. L. Sprung, E. Moya de Guerra, and M. Nishimura, *Nucl. Phys. A* 483 (1988) 77.
- [49] P. Sarriguren, E. Graca, D. W. L. Sprung, E. Moya de Guerra, and D. Berdichevsky, *Phys. Rev. C* 40 (1989) 1414.
- [50] E. Moya de Guerra, P. Sarriguren, J. A. Caballero, M. Casas, and D. W. L. Sprung, *Nucl. Phys.* **A529**, 68 (1991).
- [51] P. Sarriguren, D. Merino, O. Moreno, E. Moya de Guerra, D. N. Kadrev, A. N. Antonov, and M. K. Gaidarov, *Phys. Rev. C* 99 (2019) 034325.
- [52] B. Hernandez, P. Sarriguren, O. Moreno, E. Moya de Guerra, D. N. Kadrev, and A. N. Antonov, *Phys. Rev. C* 103 (2021) 014303.
- [53] H. de Vries, C. W. de Jager, and C. de Vries, *At. Data Nucl. Data Tables* 36 (1987) 495.
- [54] H. Euteneuer, H. Rothhaas, O. Schvrentker, J. R. Moreira, C. W. de Jager, L. Lapikas, H. de Vries, J. Flanz, K. Itoh, G. A. Peterson, D. V. Webb, W. C. Barber, and S. Kowalski, *Phys. Rev. C* 16 (1977) 1703.
- [55] H. Crannell, R. Helm, H. Kendall, J. Oeser, and M. Yearian, *Phys. Rev.* 121 (1961) 283; *Phys. Rev.* 123 (1961) 923.
- [56] P. Sarriguren, in preparation.